6 THE FIBER/MATIX INTERFACE

THE FIBER/MATRIX INTERFACE

Adhesion between fiber and matrix is controlled by properties of the interface. Generally high degree of adhesion is desirable to provide efficient transfer of load between fiber and matrix. The strength of the adhesion controls properties of composite in direction transverse to fibers as well as the shear properties. Strong adhesion also reduces susceptibility of the composite to environmental degradation. On the other hand poor adhesion between fiber and matrix provides higher fracture toughness for crack normal to reinforcement and minimizes tri-axial state of stress in matrix between fibers thus promoting ductility in the matrix.

Interfacial bonding

The degree of adhesion between fiber and matrix is often controlled by the surface tension. High degree of wetting between fiber and matrix promotes good bonding. Wetting is measured by the angle of contact between the matrix and the fiber when the matrix is in the liquid state. Fig. 6-1 shows the relation between surface tension among the three phases.

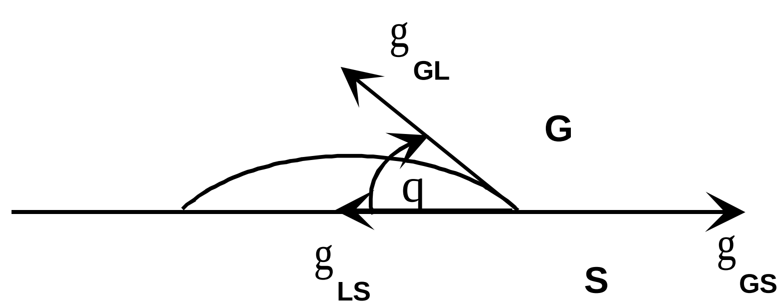

Figure 6-1 Surface tensions at solid, liquid gas interface

The surface tension between the gas and solid phase, g_{GS} is balanced by the surface tension between the liquid and solid phases, g_{LS} and the surface tension between the gas and liquid phase, g_{GL} according to

$$g_{GS} = g_{LS} + g_{LG} \cos q$$

where q is the wetting angle. Complete wetting occurs if $q = 0^\circ$ while total non-wetting occurs when $q = 180^\circ$. The wetting is influenced primarily by temperature, matrix and fiber composition.

The fiber-matrix bond strength of a composite can be measures by a several techniques. The most fundamental measure is a micro- or nano-indentation approach in which a fine probe compresses a fiber supported in the matrix as illustrated in Fig. 6-2. If the interfacial bonding is strong the shear strength between the fiber and the matrix is not exceeded the matrix will undergo compression as the fiber is compresses. If the interfacial bonding is weak the fiber will slide past the matrix producing little or no matrix compression. This effect can also occur if the composite is cooled and the constituents have difference coefficients of thermal expansion. Interfacial strength is readily reflected in the shear strength properties of practical sized specimens such as in short beam shear test shown in Fig. 6-3. In this test a beam the ratio of the

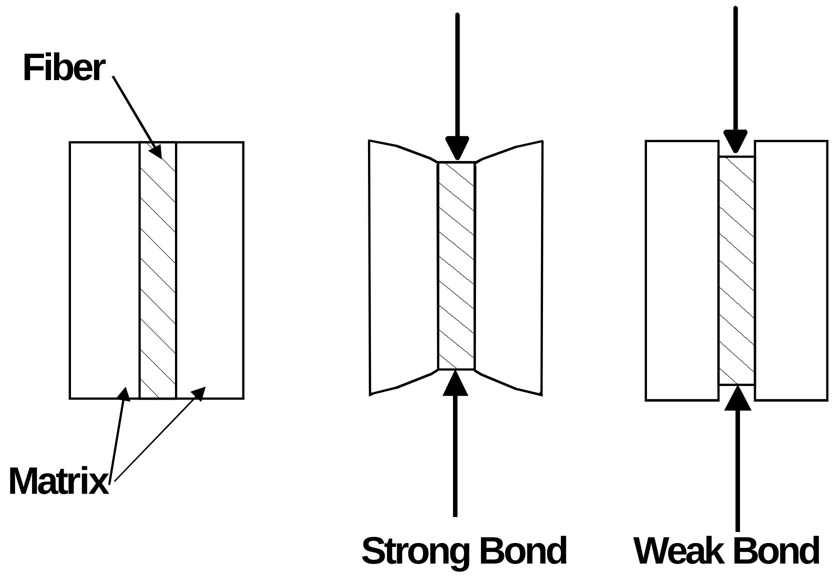

Figure 6-2 Fiber indentation test beam

depth to support length is large. A strong interfacial bond results in the beam fracturing through the beam depth even though the fibers are normal to the crack propagation direction. In a composite with a weak interface the beam will split longitudinally.

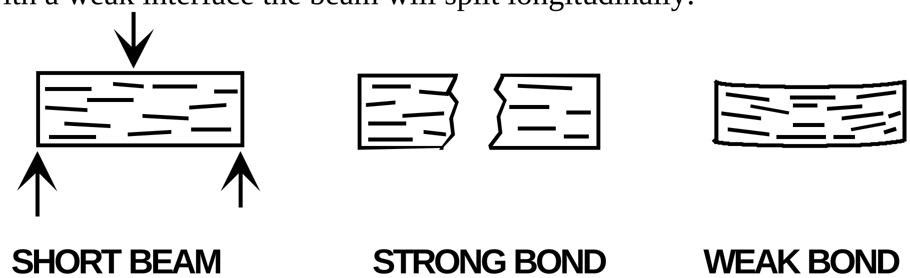

Figure 6-3. Effect of interfacial bond strength on the short beam shear test.

By performing a direct shear test, such as the Iosipescu shear test shown in Fig.6-4, the interfacial bond strength can be related to the direction of shear through the specimen. Strong interfacial bonding results in sufficient shear strength to resist the longitudinal propagation of the shear crack. In this case the crack takes the shorter path at 45^{o} to the load direction, thus breaking off the corner of the specimen. If the interfacial bonding is weak the crack propagates more or less in the load direction, possibly deviating only enough to fine the weakest fiber matrix interface.

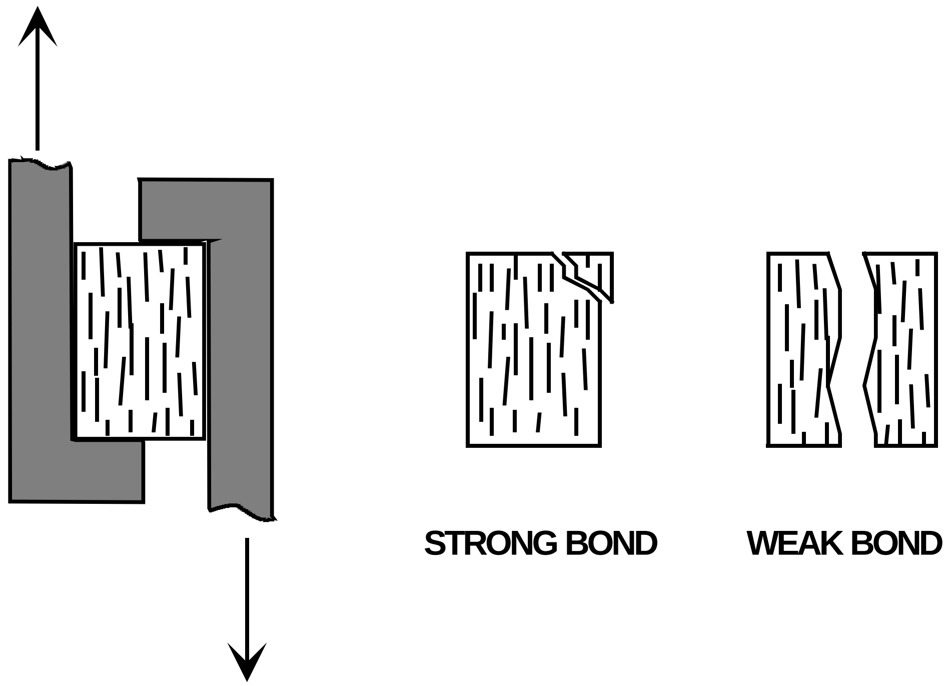

Figure 6-4 Effect of interfacial bond strength on Iosipescu shear test.

<u>DIRECT EFFECT OF INTERFACIAL BONDING</u>

The effects of interfacial bond strength can be seen composite beam thickness, Young's modulus, and interfacial failure.

Effect on bending stiffness

The effect of fiber-matrix bond strength on the bending of a composite beam can be understood by examining the case when the fibers are totally unbonded to the matrix and comparing to the case of the fibers well bonded to the matrix. Consider a beam shown in fig.6-5, composed of fibers of diameter, *d.* The through the depth of the beam there are *n* such fibers and in the across the width there are *m* fibers.

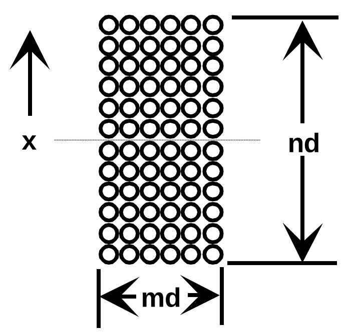

Figure 6-5 Composite beam consisting of *n* row and *m* columns of fibers.

When the fibers are totally unbonded to the matrix, presence of the matrix can be neglected, if we assume that the fiber stiffness is much greater than the matrix stiffness which is the case for polymer matrix composites. In this case the bending stiffness of the beam, D_u is the moment of inertial of each fiber times the Young's modulus of fibers, E_f times the total number of fibers

$$D_u = \frac{p\,d^4}{64} \cdot E_f \cdot mn \tag{6.1}$$

If the fibers are bonded to the matrix the bending stiffness is the product the Young's modulus of the composite and the moment of inertia of the beam

$$D_b = \left[E_f \frac{mn\left(\frac{p\,d^2}{4}\right)}{md \cdot nd} + E_m \left(1 - \frac{mn\left(\frac{p\,d^2}{4}\right)}{md \cdot nd} \right) \right] \int_{nd/2}^{-nd/2} x^2 dA$$

which evaluates to

$$D_b = \left[E_f \left(\frac{p}{4}\right) + E_m \left(1 - \frac{p}{4}\right) \right] \frac{mn^3 d^4}{12} \tag{6.2}$$

We can now estimate the ratio of the beam stiffness with bonded and unbonded fibers in a composite where the fiber stiffness exceeds the matrix stiffness by an order of magnitude such as would be the case for a carbon fiber and epoxy matrix. Neglecting the stiffness of the matrix the ratio of Eqns. (6.2) and (6.1)

$$\frac{D_b}{D_u} = \frac{4}{3} n^2$$

Effect of unbonded fibers on composite Young's modulus

Fibers that are unbonded act as if they are missing form the composite, since load cannot be transferred to and from them. The Young's modulus of a composite with a volume fraction of unbonded fibers given as V_f^* is then

$$E_c^* = E_f V_f + E_m \left(1 - V_f\right) - E_f V_f^* \tag{6.3}$$

If the stiffness of the matrix is neglected Eqn.(6.3) becomes

$$\frac{E_c^*}{E_c} = 1 - \frac{V_f^*}{V_f} \tag{6.4}$$

Eqn.(6.4) is plotted in Fig. 6-6 for various amounts of unbonded fibers. Unbonded fibers can severely reduce the composite Young's modulus with as little as 5% unbonded fibers. As the fraction of unbonded fibers increases the reduction in Young's modulus becomes severe.

Analysis of interfacial shear

Interfacial shear can be analyzed by considering the equilibrium forces on an element in a beam supported at its ends and loaded uniformly, as shown in Fig.6-7. The moment across the element, dx is

$$Vdx = M_B - M_A \tag{6.5}$$

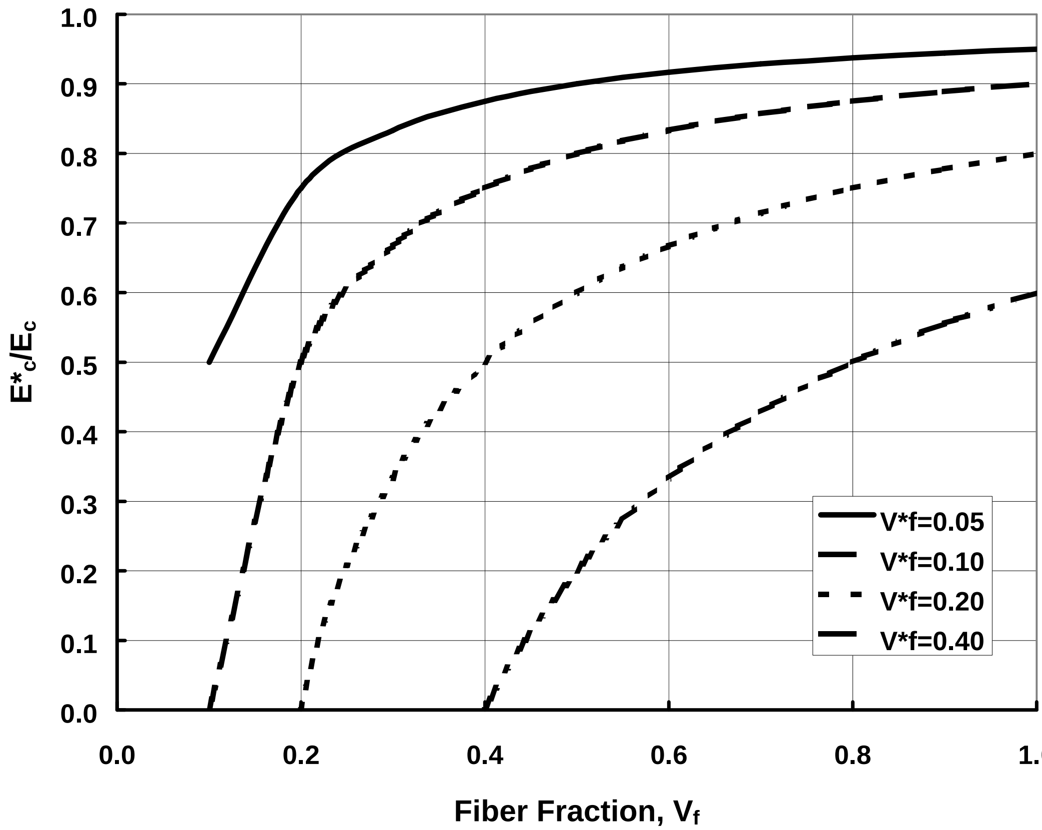

Figure 6-6 Effect of unbonded fibers on composite Young's modulus

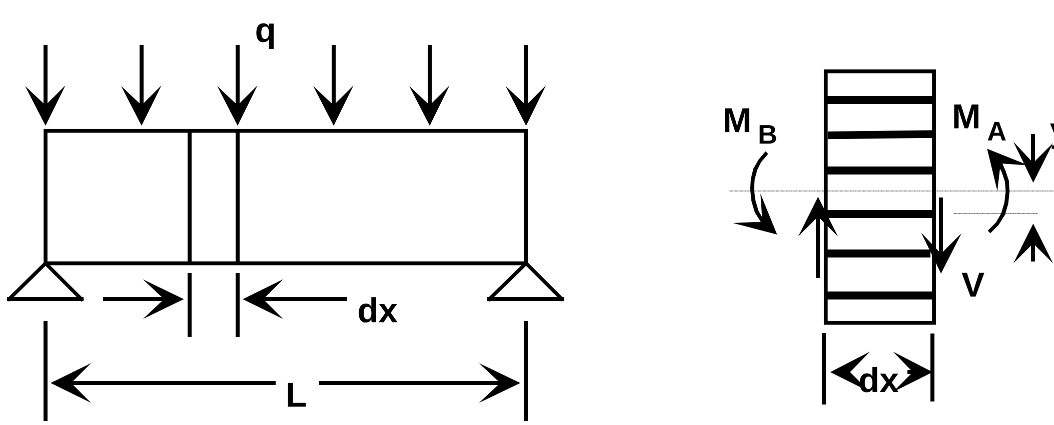

Figure 6-7 Forces on a composite beam

where V is the shearing force. Using the bending stress in the beam and the rule-of-mixtures, the stress on a fiber in the beam is

$$s_f = \frac{E_f My}{E_c I} \qquad (6.6)$$

The equilibrium forces on a fiber with a radius, r , at some depth y form the neutral axis of the composite beam, as illustrated in Fig. 6-8, can be determined by balancing the shear forces on the fiber surface, t and the tensile forces on the fiber P

$$P_{f_B} - P_{f_A} = t\,2p\,rdx \tag{6.7}$$

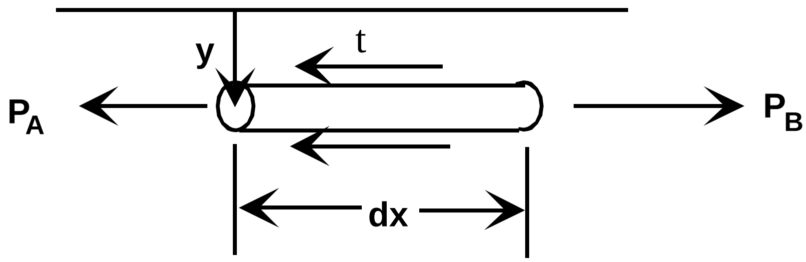

Figure 6-8 Force balance on fiber in a composite beam.

Dividing Eqn.(6.7) by the cross sectional area of the fiber, gives the stress on the fiber

$$s_f = \frac{t\,2dx}{r} \tag{6.8}$$

The ratio of fiber shear stress to tensile stress in terms of bending moment and shear forces can be obtained by using Eqns. (6.5), (6.6) and (6.7) in Eqn. (6.8)

$$\frac{t}{s_f} = \left(\frac{V}{M}\right)\left(\frac{r}{2}\right) \tag{6.9}$$

Using Eqn. (6.9) for a simply supported beam of length, L loaded at the center, see Fig.6-9, then

$$t = \left(\frac{r}{L}\right)\left(\frac{E_f}{E_c}\right)s_c$$

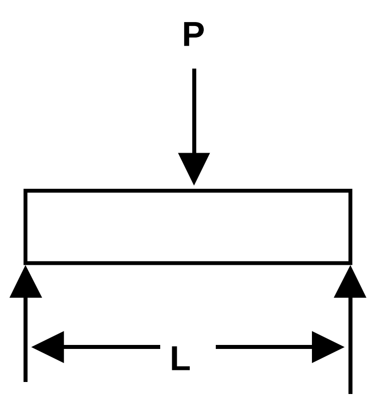

Figure 6-9 Simply supported beam loaded in the center

COMPRESSIVE LOADING OF COMPOSITES

When a composite is loaded compressively in the longitudinal direction failure can occur by a number of mechanisms including buckling, transverse splitting and shear. In addition to structural elastic buckling the fibers can undergo microbuckling that can lead to internal failure.

Microbuckling

For long slender columns two modes of microbuckling are possible depending on the volume fraction of fibers. These two modes are illustrated in Fig. 6-10. At low fiber fractions compressive loading in the longitudinal direction can cause the fibers to buckle out of phase with each other (Fig.6-10a). The matrix on the side of the fibers that are opposing concave bows are in tension while the matrix between the convex side of the fibers are in compression. Since the stresses are transverse to the fibers the composite can fail by transverse tension. The compressive strength decreases rather shapely with

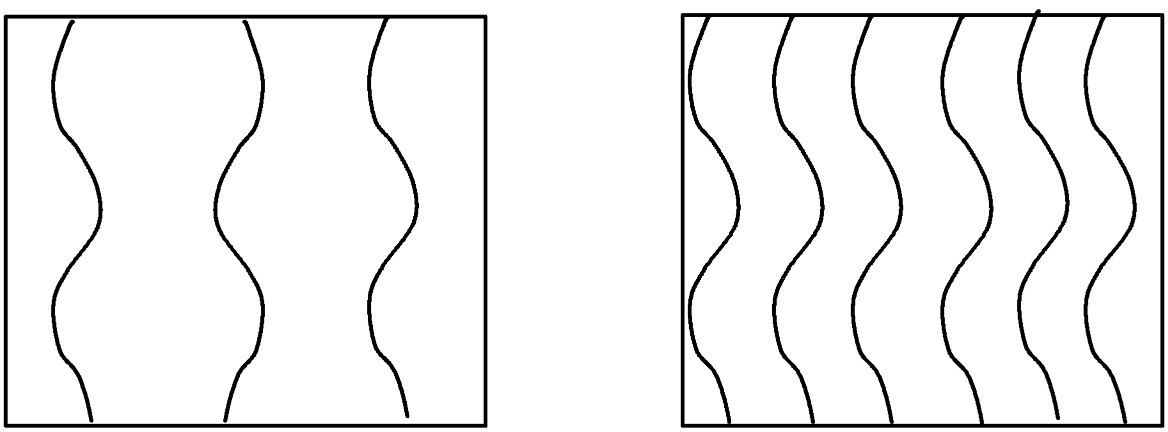

a) Extensional Mode - occurs at small V_f b) Shear Mode - occurs at large V_f

Figure 6-10 Two modes of microbuckling in composites

decreasing fiber fraction. If the fibers buckle in phase with one another as shown in Fig 6-10b the composite buckles in the shear mode. This mode is more common and can occur over a large range of fiber fractions. The compressive strength for this mode also decreases with decreasing fiber fraction but not as rapidly as for the extensional mode. For shorter columns a compressive load can cause splitting near the outer surfaces. This is due to transverse radial strains due to Poisson's expansion producing transverse tensile stresses. This mode of failure is shown in Fig.6-11. The compressive strength by extensional mode microbuckling is given by

$$s'_{LU} = 2V_f \left[\frac{V_f E_m E_f}{3(1-V_f)} \right]^{1/2} \quad (6.10)$$

In the shear mode microbuckling the compressive strength is

$$s'_{LU} = \frac{G_m}{1 - V_f} \tag{6.11}$$

It is clear that this mode of compressive failure is promoted by low matrix shear strength.

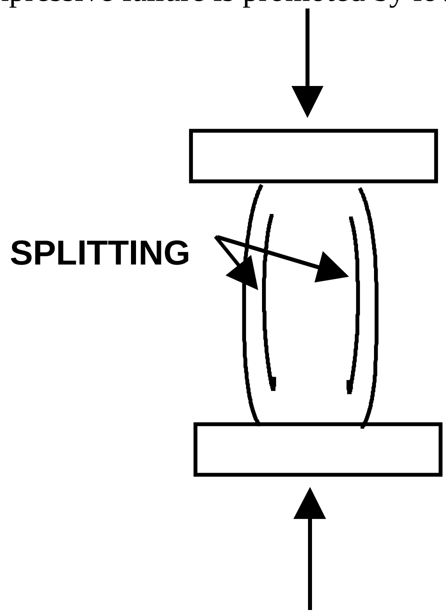

Figure 6-11 Transverse splitting mode for short columns in compression

In the splitting mode of failure transverse strain is depends upon the Poisson's ratio,

$$e_T = -e_L n_{LT}$$

The transverse failure strain is then

$$e_{TU} = \frac{s'_{LU} n_{LT}}{E_c} \tag{6.12}$$

solving for the compressive strength

$$s'_{LU} = \frac{E_c e_{TU}}{n_{LT}} \tag{6.13}$$

Eqn. (6.13) can be expressed in terms of the rule-of-mixtures values for E_c and n_{LT} , and the empirical approximation for e_{TU}

$$s'_{LU} = \frac{\left(E_f V_f + E_m V_m\right) e_{mu} (1 - V_f^{1/3})}{n_f V_f + n_m V_m} \tag{6.14}$$

A comparison of the longitudinal compressive failure strength for these three modes is shown in Fig 6-12. for a typical carbon fiber – epoxy matrix composite. The extensional and shear buckling are based on elastic instability therefore the values at high fiber fractions are not realistic. The strengths are plotted in logarithmic scale for visual resolution. It can be seen from this figure that at fiber fractions below 0.12 extensional bucking is the most likely failure mode. From 0.12 to 0.62 fiber fraction shear buckling is the most likely compressive failure mode. Above 0.62 fiber fraction transverse splitting is the dominant compressive failure mode.

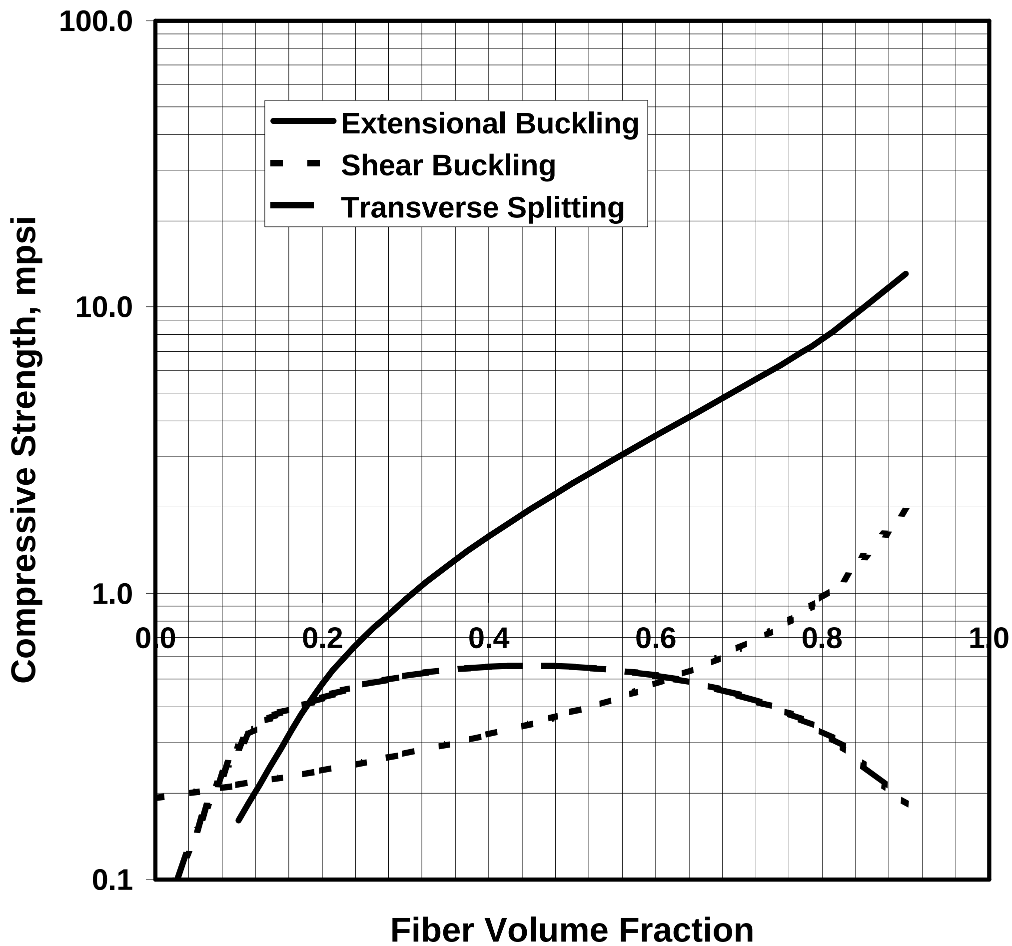

Figure 6-12. Comparison of three longitudinal compressive failure modes

Carbon fiber composites are susceptible to shear failure in which the fibers form kink bands in the 45º shear path of the matrix. This failure mode is depicted in Fig. 6-13. The kink band is formed by the local rotation of the fiber. Carbon fibers are analogous to chains that are very stiff when extended in tension but buckle easily in compression.

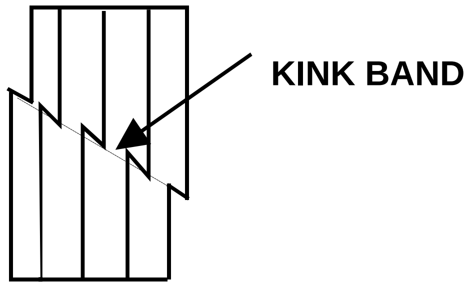

Figure 6-13 Shear failure in carbon fiber composites

Other failure modes sensitive to interfacial strength

Transverse tensile failure, and transverse compressive failure are both very sensitive to interfacial bond strength. In the case of transverse tension, debonding is the primary mode of failure. When the interfacial strength is great the either the matrix with fracture or the fibers will split longitudinally. In the case of transverse compression the weak interface promotes sliding of the fiber along the matrix. For strong interfacial strength, either the matrix shears or the fibers can be crushed. In-plane shear is also promoted by weak interfacial bond where the fibers and matrix will slide past each other easily.

Design consideration

The strength calculations for compressive loading discussed above are valid for short columns only. When the columns are sufficiently long failure will occur by gross buckling instability. The gross buckling phenomenon will occur when the critical slenderness ratio, $(L/r)_{crit}$, is exceeded. To determine this limit one can make use of the Euler equation

$$\frac{P}{A} = \frac{C\pi^2 E}{(L/r)^2} \tag{6.15}$$

where P is the buckling load, C is the coefficient of constraint, E is Young's Modulus, L is the length of the column, A is the cross section area and r is the least radius of gyration given by $\sqrt{I/A}$. Figure 6-14 shows the relation between the load per unit area and the slenderness ratio for a typical fiber glass composite. For a given short column with a failure stress, s'_{LU} , the critical slenderness ratio is given as

$$\left(\frac{L}{r}\right)_{crit} = \sqrt{\frac{Cp^2 E_c}{s'_{LU}}} \tag{6.16}$$

The critical slenderness ratio, depends upon the compressive strength of the rod. For a metal rod yield strength would determine the critical slenderness ratio since compressive yielding would be the failure mode for a short column. For fiber composites the failure mode depends upon the fiber volume fraction. For a high fiber fraction composite, the compression failure would be by transverse splitting and the short column compressive strength would be given as

$$s'_{LU} = \frac{\left(E_f V_f + E_m(1-V_f)\right) s_{mu}(1-V_f^{1/3})}{E_m(n_f V_f + n_m(1-V_m))} \tag{6.17}$$

Combining Equations 6.16 and 6.17 the critical buckling ratio for transverse splitting is then

$$\left(\frac{L}{r}\right)_{crit} = \sqrt{\frac{Cp^2 E_m n_c}{s_{mu}\left(1-V_f^{1/3}\right)}} \tag{6.18}$$

For intermediate fiber fractions microbuckling by shear mode is the compressive failure mechanism and the critical slenderness ratio can be found by combining Equations 6.11 and 6.16

$$\left(\frac{L}{r}\right)_{crit} = \sqrt{\frac{Cp^2 E_c(1-V_f)}{G_m}} \tag{6.19}$$

For low fiber fraction extensional microbuckling prevails and the critical slenderness ratio is found by combining Equations 6.10 and 6.16

$$\left(\frac{L}{r}\right)_{crit} = \sqrt{\frac{Cp^2 E_c\sqrt{3\left(1-V_f\right)}}{2V_f\sqrt{V_f E_m E_f}}} \tag{6.20}$$

Let us examine the short column failure modes for an S-glass fiber composite in a polyester flexible thermoset matrix (Figure 6-14). From this figure we can determine that the extensional microbuckling phenomenon will prevail up to 7% fiber content. The shear microbuckling mode will occur for 7% to 88% fiber content and the transverse splitting mode will occur above that.

We can consider three composites each with a fiber content where a different failure mode prevails, say 5%, 65% and 88%. Figure 6-15 shows the buckling load/unit area as predicted by the Euler formula for each fiber fraction and failure mode. The critical buckling ratio for each case can be determined using Equations 6.18 through 6.20.

These slenderness ratios were based on calculated compressive strength. Where experimental compressive strengths are available Equation 6.16 should be used. The critical slenderness ratios of some common composites determined from experimentally available compressive strengths are shown in Figure 6-16.

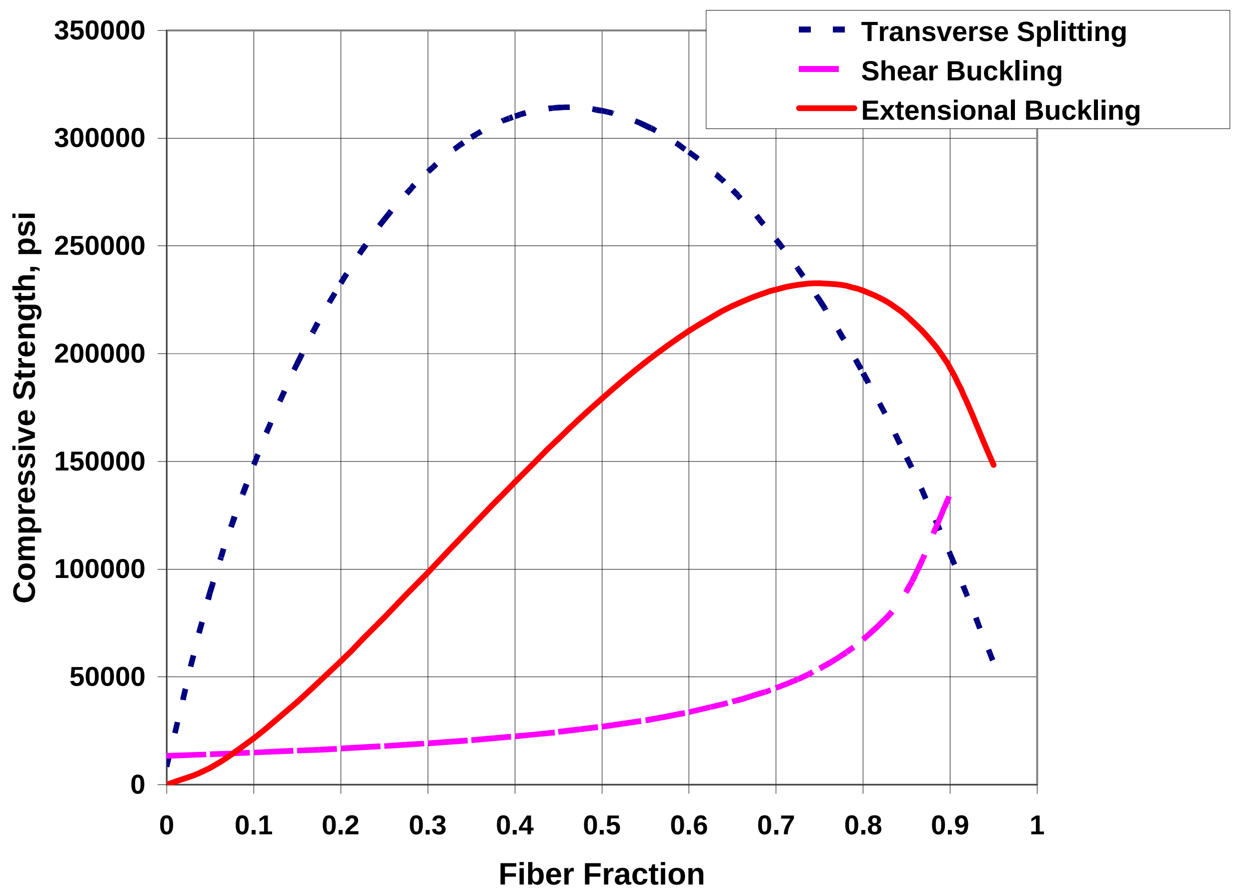

Figure 6-14. Compressive failure for S-glass/polyester flexible thermoset composite.

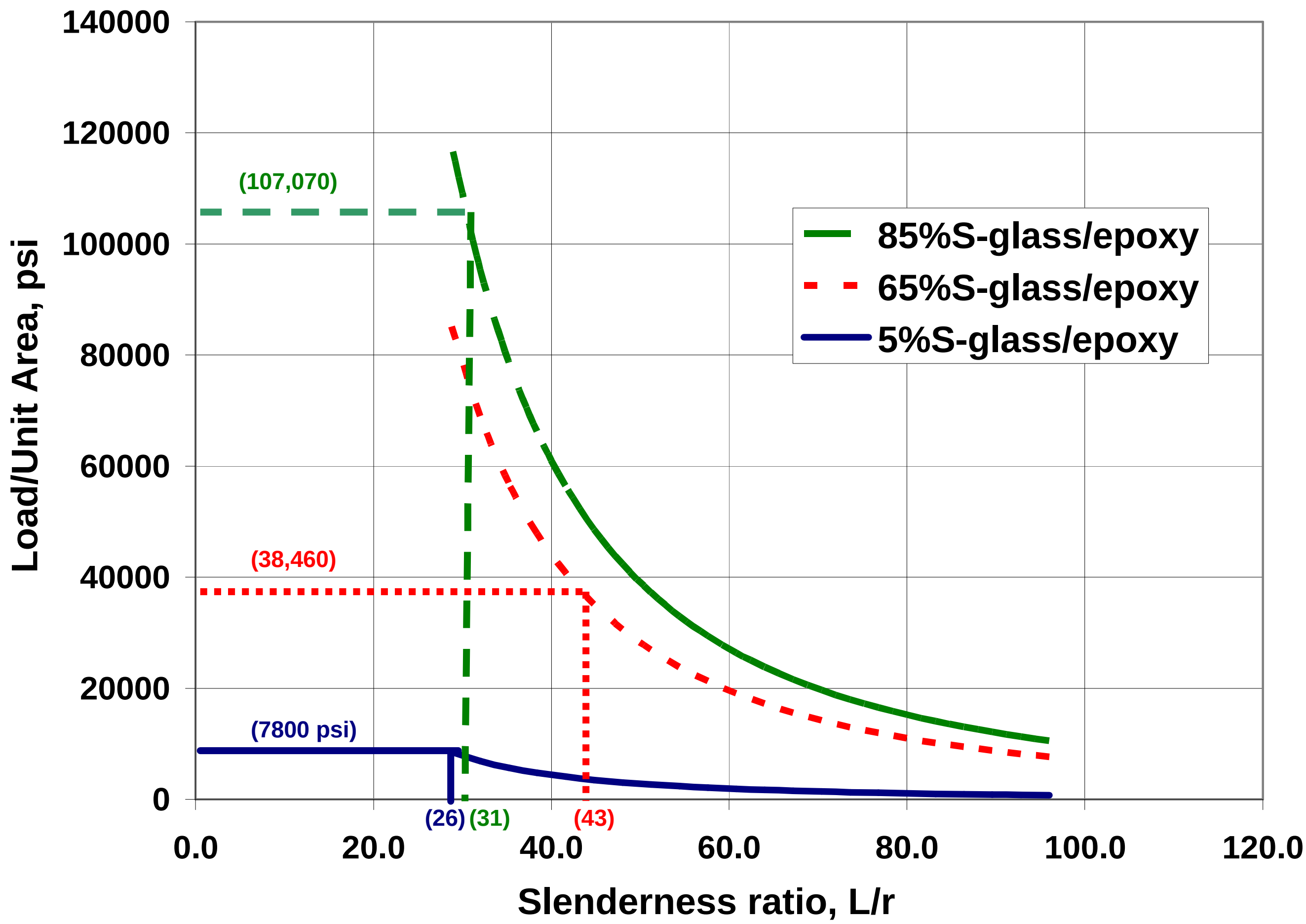

Figure 6-15 Critical slenderness ratios for various S-glass/polyester composites

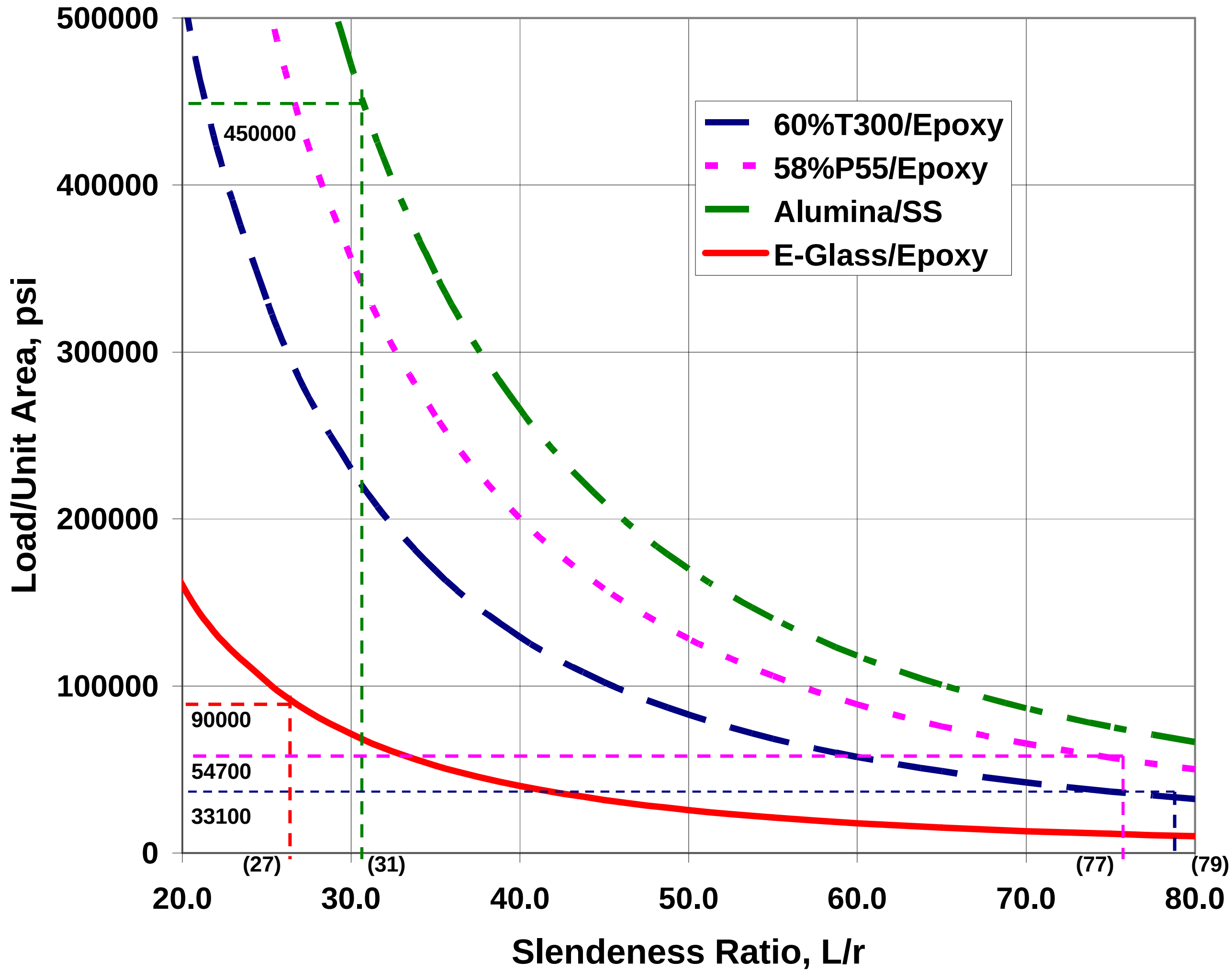

Figure 6-16 Critical slenderness ratios computed from experimentally determined compressive strengths.

Exercise Problems

1. What is the compressive failure load and mode of failure of a square rod (15 mm wide by 250 mm long composed of 49% by volume Boron monofilaments in an Al 6061 alloy in which the fibers are in the long direction. (Assume and end constraint coefficient of 1)

Constituent	Young's Modulus, GPa	Poisson's Ratio	Yield Strength, MPa
Boron monofilament	393	0.20	-
Al 6061 alloy	70	0.33	213.8